Transient magnetoconductivity of photoexcited electrons

O.E. Raichev and F.T. Vasko*

Institute of Semiconductor Physics,

National Academy of Sciences of Ukraine,

Prospekt Nauki 45, Kiev, 03028, Ukraine

(Dated: February 6, 2008)

Abstract

Transient magnetotransport of two-dimensional electrons with partially-inverted distribution excited by an ultrashort optical pulse is studied theoretically. The time-dependent photoconductivity is calculated for GaAs-based quantum wells by taking into account the relaxation of electron distribution caused by non-elastic electron-phonon interaction and the retardation of the response due to momentum relaxation and due to a finite capacitance of the sample. We predict large-amplitude transient oscillations of the current density and Hall field (Hall oscillations) with frequencies corresponding to magnetoplasmon range, which are initiated by the instability owing to the absolute negative conductivity effect.

PACS numbers: 73.50.Jt, 73.50.Pz, 73.50.Bk

*Electronic address: ftvasko@yahoo.com

I. INTRODUCTION

The transient process under an abrupt turn on of the electric current through a conducting sample is described by a simple exponential dependence if the applied voltage is fixed, i.e. the load resistance is small and the circuit effects are not essential. The characteristic temporal scale of this process is determined by the momentum relaxation time, which depends on the average energy of electrons and on the mechanisms of electron scattering.[1,2] Such kind of exponential relaxation of electric current in pure bulk Ge has been demonstrated more than 30 years ago.[3] To investigate the transient processes, one can use ultrafast photoexcitation of carriers instead of an abrupt switching of the applied voltage. Since this excitation creates non-equilibrium electrons inside the conduction band, the temporal dependence of the current contains a slow component reflecting the energy relaxation of these electrons owing to quasielastic scattering by acoustic phonons. This slow energy relaxation, corresponding to the temporal scale which is much larger than the momentum relaxation time, takes place for the electrons in the passive region (i.e. for the electrons whose energies ε are smaller than the optical phonon energy $\hbar\omega_o$), because the interaction of these electrons with optical phonons can be neglected at small temperatures $T \ll \hbar\omega_o$. The slow temporal dependence of the transient photocurrent in this case occurs for the same reason as the dependence of the photocurrent on the excitation energy under stationary photoexcitation.[4]

If the energies of excited electrons are close to $\hbar\omega_o$, see the initial distribution B in Fig. 1 (a), the absolute negative conductivity (ANC) should take place, because the non-equilibrium distribution f_ε of electrons in the passive region becomes inverted ($\partial f_\varepsilon/\partial\varepsilon > 0$) in a certain interval of energies near the upper boundary of this region. Though such a possibility has been discussed a long time ago[5] for the regime of stationary photoexcitation in bulk samples, the ANC effect has not been detected so far in this regime. The absence of the ANC under a stationary photoexcitation is described by accumulation of low-energy electrons with time (owing to slowness of interband recombination) so that the relative contribution of the inverted high-energy part of electron distribution to the conductivity becomes non-essential. In addition, the Coulomb scattering of high-energy electrons by the low-energy ones leads to a rapid broadening of the initial narrow distribution of photoexcited electrons in the energy space, thereby decreasing the contribution of the inverted part of electron distribution. To date, the ANC has been realized by means of electron heating by

electric field in many-valley semiconductors[6] owing to intervalley redistribution of electrons, or when acting by microwave radiation on two-dimensional (2D) electrons in a quantizing magnetic field.[7] Recently, see Refs. 8, 9 and Ch. 11 in Ref. 10, it has been shown that the transient ANC, which exists during a time interval of the order of momentum relaxation time, can be achieved by ultrafast photoexcitation of electrons with energies close to $\hbar\omega_o$. The theoretical description of this effect[9] has been based on the kinetic theory taking into account temporal non-locality of the response on the scale of momentum relaxation time and involving a detailed consideration of inelastic scattering of high-energy electrons by acoustic phonons. In this paper, we study the influence of classical magnetic fields on the transient ANC in 2D samples with the geometry of a long Hall bar, see Fig. 1 (b).

The main feature of the transient magnetotransport under consideration is the appearance of temporal oscillations of the longitudinal conductivity and transverse electric field (Hall field), whose frequencies are of the order of the cyclotron frequency ω_c (Hall oscillations). Weak oscillations of this kind should be always present in the transient response because of the retardation of charge accumulation on the sides of the Hall bar. The existence of the transient ANC leads to the instability which dramatically modifies the transient oscillations. In the initial moments of time, when the longitudinal current flows in the direction opposite to the applied field, the Hall field increases in the direction opposite to its equilibrium one, because the sign of the Lorentz force is changed in the ANC regime. For the same reason, this increase is exponential: the charge accumulation on the sides leads to further enhancement of this accumulation. In the subsequent moments of time, when the partial inversion of the electron distribution is no longer sufficient to provide the ANC, the system starts decharging, and, since the system posesses a certain inertia, there appear large-amplitude oscillations of the Hall field as well as of the longitudinal current (this current is coupled to the Hall field). Both the current and the Hall field can change their signs in the process of the oscillations. The damping of such large-amplitude oscillations proceeds slower, which makes them persistent on a nanosecond time scale.

The paper is organized as follows. In Sec. II we derive general equations for transient magnetotransport of electrons, which describe temporal dependence of the longitudinal current and Hall field. Section III is devoted to a simple model which makes it possible to solve these equations analytically and to describe the main features of the transient response. In Sec. IV we present the results of numerical calculations involving a detailed consideration of

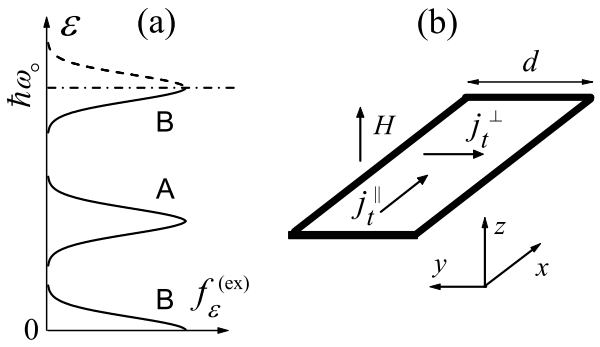

FIG. 1: (a) Initial electron energy distribution $f_\varepsilon^{(ex)}$ for the cases of excitations away from the optical phonon energy (A) and near the optical phonon energy (B). (b) Hall bar geometry and electric currents in the presence of a magnetic field H directed perpendicular to the 2D plane.

the evolution of electron distribution. The discussion of the assumptions used and concluding remarks are given in the last section. The Appendix A contains the expressions for the transition probability and relaxation rate of 2D electrons interacting with acoustic phonons. The Appendix B contains the formalism describing the retardation of charge accumulation at the sides of the Hall bar.

II. TEMPORAL RESPONSE

We describe the response of photoexcited electrons to an electric field $\mathbf{E}_t$ by representing the distribution function $f_{\mathbf{p}t}$, which depends on the electron momentum $\mathbf{p}$ and time t, in the form $f_{\mathbf{p}t} = f_{\varepsilon t} + \Delta f_{\mathbf{p}t}$, where $f_{\varepsilon t}$ is the symmetric part of this function and $\Delta f_{\mathbf{p}t}$ is the antisymmetric contribution induced by the field. Under the approximation of weak electric field, when the heating of electrons by the field is neglected, the symmetric part, which describes the energy distribution of non-degenerate electrons, is governed by the kinetic equation

$$\frac{\partial f_{\varepsilon t}}{\partial t} = J_{ac}\left(f_t \mid \varepsilon\right) + J_{opt}\left(f_t \mid \varepsilon\right). \tag{1}$$

The collision integral due to acoustic-phonon scattering, J_{ac}, can be written as

$$J_{ac}\left(f_t \mid \varepsilon\right) = \rho_{ß2D} \int_0^\infty d\varepsilon' \left[W_{\varepsilon'\varepsilon} f_{\varepsilon' t} - W_{\varepsilon\varepsilon'} f_{\varepsilon t}\right], \tag{2}$$

where $\rho_{ß2D} = m/\pi\hbar^2$ is the density of states of 2D electrons with the effective mass m. The scattering probabilities $W_{\varepsilon'\varepsilon}$ and $W_{\varepsilon\varepsilon'}$ are determined by the deformation-potential (DA) and

piezoelectric (PA) interactions of electrons with acoustic phonons, see Appendix A. These probabilities satisfy the requirement of detailed balance, $W_{\varepsilon'\varepsilon} = W_{\varepsilon\varepsilon'} \exp[(\varepsilon' - \varepsilon)/T]$, where T is the phonon temperature. The collision integral J_{opt}, which describes the interaction of non-degenerate electrons with dispersionless optical phonons at $T \ll \hbar\omega_o$, can be represented in a similar form:

$$J_{opt}\left(f_t \mid \varepsilon\right) = \nu_o \int d\varepsilon' \left[\delta\left(\varepsilon - \varepsilon' + \hbar\omega_o\right) f_{\varepsilon' t} - \delta\left(\varepsilon - \varepsilon' - \hbar\omega_o\right) f_{\varepsilon t}\right], \tag{3}$$

where ν_o is the rate of spontaneous emission of optical phonons by 2D electrons (see, for example, Ref. 10).

Since the rate ν_o is typically much larger than the rate of acoustic-phonon scattering, any electron appearing in the active region ($\varepsilon > \hbar\omega_o$) after photoexcitation or after acoustic-phonon absorption instantaneously relaxes to a state in the passive region, with the energy $\varepsilon - k\hbar\omega_o$, where k is the number of emitted optical phonons. In this approximation, the kinetic equation (1) can be considered for the passive region only. To carry out such a transformation, we first rewrite the term describing departure of electrons from the state ε in Eq. (2) as $\rho_{\text{ß}2D} \int_0^{\hbar\omega_o} d\varepsilon' \sum_{k=0}^{\infty} W_{\varepsilon\varepsilon'+k\hbar\omega_o} f_{\varepsilon t}$. Since the active region is empty owing to rapid emission of optical phonons ($f_{\varepsilon t} = 0$ at $\varepsilon > \hbar\omega_o$), this term is considered in the region $\varepsilon < \hbar\omega_o$ only. For the same reason, the term corresponding to arrival of electrons at the state ε in Eq. (2) is written as $\rho_{\text{ß}2D} \int_0^{\hbar\omega_o} d\varepsilon' W_{\varepsilon'\varepsilon} f_{\varepsilon' t}$. This term describes transitions of electrons both to the states with $\varepsilon < \hbar\omega_o$ and to the states with $\varepsilon > \hbar\omega_o$. As explained above, in the latter case the electrons instantaneously relax to the states with the energies $\varepsilon - k\hbar\omega_o$ in the passive region. Therefore, in the presence of rapid spontaneous emission of optical phonons the arrival term takes the form $\rho_{\text{ß}2D} \int_0^{\hbar\omega_o} d\varepsilon' \sum_{k=0}^{\infty} W_{\varepsilon'\varepsilon+k\hbar\omega_o} f_{\varepsilon' t}$, where $\varepsilon < \hbar\omega_o$. Finally, since $W_{\varepsilon\varepsilon'}$ becomes exponentially small at $\varepsilon' - \varepsilon > \hbar\omega_o$, see Appendix A, one should retain only the terms with $k = 0$ and $k = 1$ both in the arrival and in the departure terms. As a result, Eq. (1) is reduced to the following form:

$$\frac{\partial f_{\varepsilon t}}{\partial t} = \rho_{\text{ß}2D} \int_0^{\hbar\omega_o} d\varepsilon' \left[(W_{\varepsilon'\varepsilon} + W_{\varepsilon'\varepsilon+\hbar\omega_o}) f_{\varepsilon' t} - (W_{\varepsilon\varepsilon'} + W_{\varepsilon\varepsilon'+\hbar\omega_o}) f_{\varepsilon t}\right]. \tag{4}$$

The term with $W_{\varepsilon'\varepsilon+\hbar\omega_o}$ in this equation becomes essential only if ε' is close to $\hbar\omega_o$ and ε is close to zero. Similarly, the term with $W_{\varepsilon\varepsilon'+\hbar\omega_o}$ becomes essential if ε is close to $\hbar\omega_o$ and ε'

is close to zero.

Equation (4) should be solved with the initial condition $f_{\varepsilon t=0} = f_{\varepsilon}^{(ex)}$, where $f_{\varepsilon}^{(ex)}$ is determined by the excitation pulse. If the initial ultrafast excitation creates electrons with the distribution $F_{\varepsilon}^{(ex)}$, we have $f_{\varepsilon}^{(ex)} = \theta(\hbar\omega_o - \varepsilon)\sum_{k=0}^{\infty} F_{\varepsilon+k\hbar\omega_o}^{(ex)}$, where the terms with $k \neq 0$ describe the electrons instantaneously transferred to the passive region via optical phonon emission. Note that Eq. (4) satisfies the density conservation requirement implying that the electron density $\rho_{ß2D}\int_0^{\hbar\omega_o} d\varepsilon f_{\varepsilon t}$ does not depend on time and equal to the excited density $n_{ex} = \rho_{ß2D}\int_0^{\hbar\omega_o} d\varepsilon f_{\varepsilon}^{(ex)}$.

The weak antisymmetric part $\Delta f_{\mathbf{p}t}$, in the presence of a stationary magnetic field $\mathbf{H}$ ($\mathbf{E}\perp\mathbf{H}$), is governed by the linearized kinetic equation

$$\left(\frac{\partial}{\partial t} + \frac{e}{c}[\mathbf{v}\times\mathbf{H}]\cdot\frac{\partial}{\partial\mathbf{p}}\right)\Delta f_{\mathbf{p}t} + e\mathbf{E}_t\cdot\frac{\partial f_{\varepsilon t}}{\partial\mathbf{p}} \simeq -\nu_{\varepsilon}\Delta f_{\mathbf{p}t}, \tag{5}$$

where e is the electron charge, c is the velocity of light, and $\mathbf{v} = \mathbf{p}/m$ is the electron velocity. The momentum relaxation rate on the right-hand side of Eq. (5) is the sum of the rate of quasielastic scattering of electrons by acoustic phonons, $\nu_{\varepsilon}^{ß(ac)}$, (see Appendix A) and the rate of spontaneous emission of optical phonons, $\nu_o\theta(\varepsilon - \hbar\omega_o)$. The exact solution of Eq. (5) is given by

$$\Delta f_{\mathbf{p}t} = e\int_0^t dt'\; e^{-\nu_{\varepsilon}(t-t')}\mathbf{v}\cdot\mathbf{K}_{tt'}\left(-\frac{\partial f_{\varepsilon t'}}{\partial\varepsilon}\right), \tag{6}$$

$$\mathbf{K}_{tt'} \equiv \mathbf{E}_{t'}\cos\omega_c(t-t') + \frac{[\boldsymbol{\omega}_c\times\mathbf{E}_{t'}]}{\omega_c}\sin\omega_c(t-t'),$$

where $\boldsymbol{\omega}_c = |e|\mathbf{H}/mc$ is the cyclotron frequency vector.

The current density is given by the standard formula, $\mathbf{j}_t = (2/L^2)\sum_{\mathbf{p}}\mathbf{v}\Delta f_{\mathbf{p}t}$, where L^2 is the normalization square. Using Eq. (6) and performing the averaging over the angle of $\mathbf{p}$, we write $\mathbf{j}_t$ as

$$\mathbf{j}_t = \frac{e^2\rho_{ß2D}}{m}\int_0^t dt'\mathbf{K}_{tt'}\int_0^{\infty} d\varepsilon\varepsilon e^{-\nu_{\varepsilon}(t-t')}\left(-\frac{\partial f_{\varepsilon t'}}{\partial\varepsilon}\right). \tag{7}$$

The linear response of electron system to the electric field $\mathbf{E}_t$ is described by the time-dependent conductivity tensor $\widehat{\sigma}_{tt'}$ introduced according to the non-local relation $\mathbf{j}_t = \int_0^t dt'\widehat{\sigma}_{tt'}\mathbf{E}_{t'}$. The diagonal and non-diagonal components of this tensor, $\sigma_{tt'}^{ß\|}$ and $\sigma_{tt'}^{ß\perp}$, are

$$\left|\begin{array}{c}\sigma_{tt'}^{ß\|}\\ \sigma_{tt'}^{ß\perp}\end{array}\right| = \frac{e^2\rho_{ß2D}}{m}\left|\begin{array}{c}\cos\omega_c(t-t')\\ \sin\omega_c(t-t')\end{array}\right| \times\int_0^{\hbar\omega_o} d\varepsilon\varepsilon e^{-\nu_{\varepsilon}(t-t')}\left(-\frac{\partial f_{\varepsilon t'}}{\partial\varepsilon}\right). \tag{8}$$

The contribution of the active region is neglected in this equation, because this region is depleted of electrons owing to rapid emission of optical phonons. Accordingly, the scattering rate ν_ε standing in Eq. (8) is equal to the acoustic-phonon scattering rate $\nu_\varepsilon^{ß(ac)}$ calculated in Appendix A.

Below we consider a sample of Hall bar geometry, a 2D strip of width d with the in-plane current density $\mathbf{j}_t = (j_t^{ß\|},\ j_t^{ß\perp})$, where $\|$ and $\perp$ components of $\mathbf{j}_t$ are referred to the coordinate system associated with the geometry of the Hall bar (Fig. 1 b). The transverse current density $j_t^{ß\perp}$ is not equal to zero and describes the transient process of charge accumulation on the sides (edges) of the Hall bar. Owing to near-edge localization of the magnetoinduced charges and current continuity, one can use the homogeneous current vector. Under the assumption of high resistance of the photoexcited electron gas in comparison to the load resistance of the circuit, we have $\mathbf{E}_t = (E^{ß\|}, E_t^{ß\perp})$, where the longitudinal field $E^{ß\|}$ is determined by the applied voltage and remains time-independent. The Hall field $E_t^{ß\perp}$ depends on time because of the charge accumulation process mentioned above. The components of the current density vector are written through the components of conductivity tensor (8) as follows:

$$j_t^{ß\perp} = \int_0^t dt' \left(\sigma_{tt'}^{ß\|} E_{t'}^{ß\perp} + \sigma_{tt'}^{ß\perp} E^{ß\|}\right), \tag{9}$$

$$j_t^{ß\|} = \int_0^t dt' \left(\sigma_{tt'}^{ß\|} E^{ß\|} - \sigma_{tt'}^{ß\perp} E_{t'}^{ß\perp}\right) \equiv \sigma_t^{ßeff} E^{ß\|}, \tag{10}$$

where we have introduced the effective conductivity $\sigma_t^{ßeff}$. To obtain a closed equation for the Hall field, one should describe the charge accumulation at the sides of the Hall bar. This leads to the approximate equation

$$j_t^{ß\perp} \simeq -C_{ß\perp} \frac{dE_t^{ß\perp}}{dt}, \tag{11}$$

where $C_{ß\perp} = \alpha\epsilon d$ is the effective capacitance proportional to the dielectric permittivity ϵ, and α is a small numerical factor. The derivation of Eq. (11) and the estimate of α are given in Appendix B.

In summary, to describe the linear response of the system, one has first to solve Eq. (4) and determine the energy distribution $f_{\varepsilon t}$. Then, $\sigma_{tt'}^{ß\|}$ and $\sigma_{tt'}^{ß\perp}$ are calculated according to Eq. (8). Using them in Eq. (9) and applying Eq. (11), one finds the Hall field $E_t^{ß\perp}$, which is proportional to the time-independent longitudinal field $E^{ß\|}$. Finally,

the longitudinal current is expressed through the effective conductivity from Eq. (10): $\sigma_t^{ßeff} = \int_0^t dt' \left(\sigma_{tt'}^{ß\|} - \sigma_{tt'}^{ß\perp} E_{t'}^{ß\perp}/E^{ß\|}\right)$.

III. ANALYTICAL APPROACH

Before presenting the results of numerical solution of Eq. (9), we discuss an approximation which allows one to understand essential features of the time-dependent response by means of analytical consideration. First of all, we neglect the energy dependence of the momentum relaxation time, replacing ν_ε in Eq. (8) by a constant $\nu = \nu_{\hbar\omega_o}$. Note that the calculated energy dependence ν_ε in the interval $0 < \varepsilon < \hbar\omega_o$ is not strong, except for the low-energy region (see Fig. 2). The integral over energy in Eq. (8) in this case is taken by parts, with the result

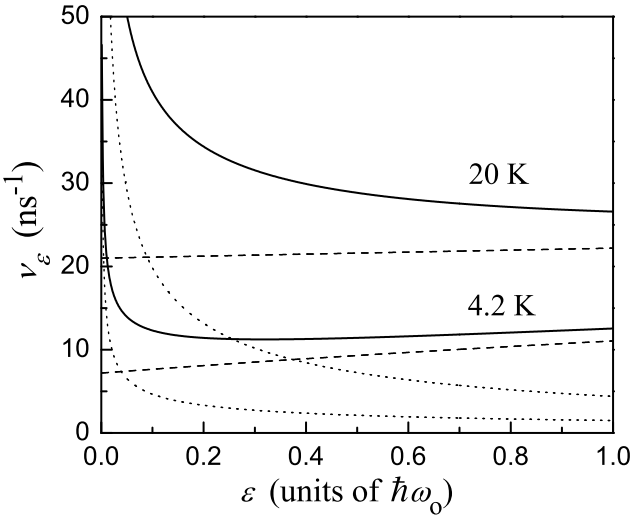

FIG. 2: Energy dependence of momentum relaxation rates for GaAs quantum well of width 10 nm for $T = 4.2$ K and $T = 20$ K. The dashed and dotted lines show the partial contributions of DA and PA scattering mechanisms, respectively.

$$\left|\begin{array}{c}\sigma_{tt'}^{ß\|}\\ \sigma_{tt'}^{ß\perp}\end{array}\right| = \frac{e^2 n_{ex}}{m}\left|\begin{array}{c}\cos\omega_c(t-t')\\ \sin\omega_c(t-t')\end{array}\right| e^{-\nu(t-t')} g_{t'} \ , \qquad (12)$$

$$g_t = \left(1 - \frac{\rho_{ß2D}\hbar\omega_o}{n_{ex}} f_{\hbar\omega_o t}\right).$$

The evolution of the energy distribution enters the conductivity tensor (12) through the dimensionless function g_t, which depends on the distribution function at the boundary of

the passive region. After substituting the expression (11) to Eq. (9) with $\sigma_{tt'}^{ß\|}$ and $\sigma_{tt'}^{ß\perp}$ given by Eq. (12), it is convenient to differentiate the equation obtained over t twice. As a result, Eq. (9) is reduced to the differential equation

$$\frac{d^3E_t^{ß\perp}}{dt^3} + 2\nu\frac{d^2E_t^{ß\perp}}{dt^2} + (\omega_c^2 + \nu^2 + \Omega^2 g_t)\frac{dE_t^{ß\perp}}{dt} + \Omega^2\left(\nu g_t + \frac{dg_t}{dt}\right)E_t^{ß\perp} + \Omega^2\omega_c g_t E^{ß\|} = 0 \tag{13}$$

with the initial conditions $E_t^{ß\perp} = dE_t^{ß\perp}/dt = d^2E_t^{ß\perp}/dt^2 = 0$ at $t = 0$. We have introduced a characteristic frequency

$$\Omega = \sqrt{\frac{e^2 n_{ex}}{mC_{ß\perp}}} \tag{14}$$

determined by the capacitance and electron density. The longitudinal current, given in the integral form by Eq. (10), can be expressed through the derivatives of $E_t^{ß\perp}$ with the use of Eqs. (9), (10), (11), and (12):

$$j_t^{ß\|} = -\frac{e^2 n_{ex}}{m\Omega^2\omega_c}\left(\frac{d^2E_t^{ß\perp}}{dt^2} + \nu\frac{dE_t^{ß\perp}}{dt} + \Omega^2 g_t E_t^{ß\perp}\right). \tag{15}$$

If the electrons are excited considerably below the optical phonon energy, see the initial distribution A in Fig. 1 (a), one has $g_t = 1$. In this case Eq. (13) is solved analytically. The solution shows a three-mode behavior according to

$$E_t^{ß\perp} = -E^{ß\|}\frac{\omega_c}{\nu}\left(1 - c_1 e^{s_1 t} - c_2 e^{s_2 t} - c_3 e^{s_3 t}\right), \tag{16}$$
$$c_1 = \frac{s_2 s_3}{(s_1 - s_2)(s_1 - s_3)}\ , \quad c_2 = \frac{s_1 s_3}{(s_2 - s_1)(s_2 - s_3)}\ ,$$
$$c_3 = \frac{s_1 s_2}{(s_3 - s_1)(s_3 - s_2)}\ ,$$

where s_{1-3} are the roots of the characteristic equation $s^3 + 2\nu s^2 + (\omega_c^2 + \nu^2 + \Omega^2)s + \nu\Omega^2 = 0$. Under the approximation $\nu^2 \ll \omega_c^2 + \Omega^2$, the solution (16) is rewritten as

$$E_t^{ß\perp} \simeq -E^{ß\|}\frac{\omega_c}{\nu}\left[1 - \exp\left(-\frac{\Omega^2}{\Omega_c^2}\nu t\right) - \frac{\Omega^2\nu}{\Omega_c^3}\exp\left(-\frac{\omega_c^2 + \Omega^2/2}{\Omega_c^2}\nu t\right)\sin(\Omega_c t)\right], \tag{17}$$

where $\Omega_c = \sqrt{\omega_c^2 + \Omega^2}$. The expression (17) describes the increase of the Hall field from 0 to its equilibrium value $-E^{ß\|}\omega_c/\nu$ with a characteristic time $(\Omega_c/\Omega)^2\nu^{-1}$ and weak oscillations of this field with the frequency Ω_c. The oscillations are exponentially damped on the time

scale of ν^{-1}, though the damping is suppressed at $(\omega_c/\Omega)^2 \ll 1$. In the case of $\omega_c \gg \Omega$, which still can be realized in the classical region of magnetic fields if the excitation density is low enough, the increase of the Hall field appears to be much slower than the damping of the oscillations. The longitudinal current shows a similar evolution, which is obvious from the relation (15).

If the electrons are excited close to the optical phonon energy (see the distribution B in Fig. 1 (a)), the function g_t is not equal to unity and can be negative at the initial moments of time, owing to the partial inversion of the electron distribution. As the excited electrons relax and go away from the boundary of the passive region, g_t changes its sign from negative to positive at some instant $t = t_0$ and approaches 1 at $t \to \infty$. Although Eq. (13) cannot be solved analytically in the general case, the basic features of the response can be determined by using the model step-like function

$$g_t = \begin{cases} g_0, & t < t_0 \\ 1, & t > t_0 \end{cases}, \tag{18}$$

where g_0 is a negative constant. Substituting the expression (18) into Eq. (13), one can find that at $t > t_0$ the solution (16) is valid again. However, the coefficients c_{1-3} should be found by means of matching this solution to the solution at $t < t_0$, which has the form

$$E_t^{ß\perp}\Big|_{t<t_0} = -E^{ß\parallel}\frac{\omega_c}{\nu}\left(1 - d_1 e^{p_1 t} - d_2 e^{p_2 t} - d_3 e^{p_3 t}\right), \tag{19}$$

and p_{1-3} are the roots of the equation $p^3 + 2\nu p^2 + (\omega_c^2 + \nu^2 + \Omega^2 g_0)p + \nu\Omega^2 g_0 = 0$. The coefficients d_{1-3} are expressed through p_{1-3} in the same way as the coefficients c_{1-3} are expressed through s_{1-3}, see Eq. (16). The rules of the matching are derived from integration of Eq. (13) across the point $t = t_0$ and imply continuity of the Hall field $E_t^{ß\perp}$ and its first time derivative, while the second derivative has a finite step, $d^2E_t^{ß\perp}/dt^2\Big|_{t=t_0-0}^{t=t_0+0} = -(1-g_0)E_{t=t_0}^{ß\perp}$, which provides the continuity of the current given by Eq. (15). It is essential that at least one of the rates p_{1-3} has a positive real part, which describes exponential increase of the Hall field in the interval $t < t_0$. This is a manifestation of the instability generated by the ANC effect. It is also important that the sign of the increasing Hall field is opposite to its equilibrium sign because of inversion of the direction of current in the ANC interval. The strong enhancement of the Hall field at $t < t_0$ initiates large-amplitude oscillations of this field (Hall oscillations) in the region $t > t_0$. The oscillations of the longitudinal current are also dramatically enhanced.

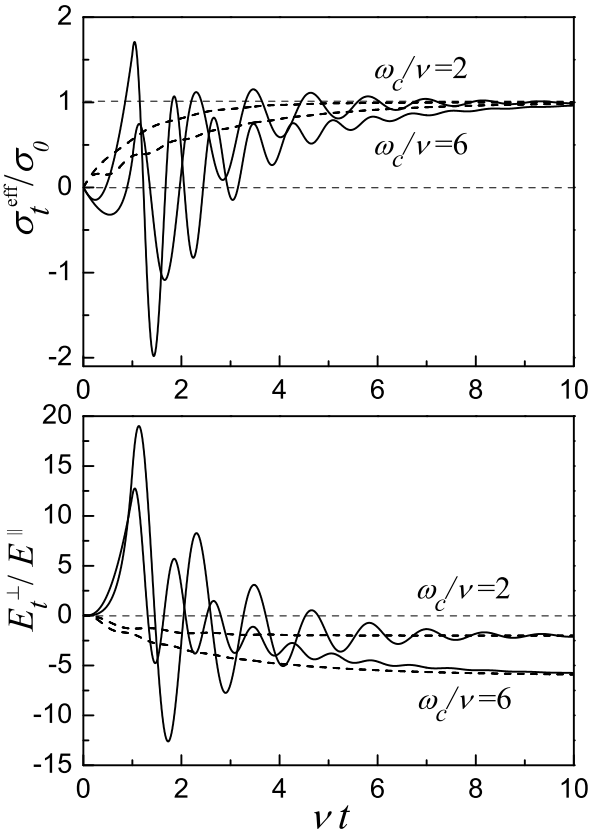

FIG. 3: Evolution of the effective conductivity $\sigma_t^{ßeff}$ and Hall field $E_t^{ß\perp}$ calculated within the approximation described by Eqs. (12) and (18) at $\Omega/\nu = 5$, $t_0 = \nu^{-1}$, and $g_0 = -1$ for two values of cyclotron frequency, $\omega_c/\nu = 2$ and $\omega_c/\nu = 6$. The dashed lines show the corresponding evolution for the case $g_t = 1$, when the excited electrons appear considerably below the optical phonon energy.

Figure 3 demonstrates some examples of temporal dependence of $E_t^{ß\perp}$ and $\sigma_t^{ßeff}$ (expressed in units of $\sigma_0 = e^2 n_{ex}/m\nu$) calculated within the analytival approach described here. We have chosen $\Omega/\nu = 5$, $t_0 = \nu^{-1}$ and $g_0 = -1$. For comparison, we also plot the corresponding temporal dependence at $g_t = 1$, when the electrons are excited below the optical phonon energy. The oscillations in this case also exist, but they are weak and superimposed on a smooth exponential relaxation dependence. On the other hand, the oscillations generated by the ANC instability are strong and remain visible even at $\nu t \simeq 10$. Estimating $\nu \simeq 12$ ns^{-1}, see Fig. 2 for 4.2 K, one can conclude that these oscillations persist over a nanosecond interval of time after the excitation. The frequency of the oscillations increases with the increase of the magnetic field and is estimated as $\Omega_c = \sqrt{\omega_c^2 + \Omega^2}$. According to

Eq. (14) and to the estimate of $C_{ß\perp}$, the frequency Ω is of the order of 2D plasmon frequency ω_q at wavenumbers q corresponding to the inverse width of the Hall bar, $q \sim 1/d$. For this reason, Ω_c is identified with a 2D magnetoplasmon frequency. The appearance of the large-amplitude Hall oscillations can therefore be considered as excitation of 2D magnetoplasmons owing to the ANC instability. The amplitude of the oscillations exponentially increases with the increase of the frequency Ω and with the increase of the absolute value of g_0. We also note that the parameters used in the calculations are physically reasonable. Indeed, if $\nu \simeq 12$ ns^{-1} (Fig. 2), then $\Omega/\nu = 5$ corresponds, for example, to $C_{ß\perp} \simeq 0.1$ cm and $n_{ex} \simeq 10^{11}$ cm^{-2} (or $C_{ß\perp} \simeq 0.01$ cm and $n_{ex} \simeq 10^{10}$ cm^{-2}) for GaAs wells, while the ratios $\omega_c/\nu = 2$ and $\omega_c/\nu = 6$ approximately correspond to the classical magnetic fields of 0.01 T and 0.03 T, respectively.

IV. NUMERICAL RESULTS

The model consideration given above ignores a detailed evolution of electron distribution after the photoexcitation. Below we present the results of a careful consideration based on the numerical solution of Eq. (9) with $\sigma_{tt'}^{ß\|}$ and $\sigma_{tt'}^{ß\perp}$ given by Eq. (8). We have used standard material parameters of GaAs, which can be found, for example, in Refs. 1 and 11 (see also our paper, Ref. 9). To find the electron distribution $f_{\varepsilon t}$ from Eq. (4), we assume that the optical pulse creates electrons with a Gaussian energy distribution $F_\varepsilon^{(ex)} \propto \exp[-(\varepsilon - \varepsilon_{ex})^2/\Delta^2]$ of a characteristic half-width Δ, centered at the excitation energy ε_{ex}. Assuming, for example, that $\varepsilon_{ex} = \hbar\omega_o$ and $(\Delta/\hbar\omega_o)^2 \ll 1$, we obtain the initial electron energy distribution in the passive region in the form of two half-peaks also shown in Fig. 1 (a):

$$f_\varepsilon^{(ex)} \propto \exp[-(\varepsilon - \hbar\omega_o)^2/\Delta^2] + \exp[-\varepsilon^2/\Delta^2], \tag{20}$$

see the discussion after Eq. (4). The numerical solution of Eq. (4) has been carried out by iterations in the time domain. The evolution of the electron distribution, calculated for 10 nm wide GaAs quantum well at 4.2 K, is shown in Fig. 4. This evolution is similar to that calculated for bulk samples in Ref. 9.

Figure 5 shows the temporal dependence of the effective conductivity $\sigma_t^{ßeff}$ and Hall field $E_t^{ß\perp}$ for 10 nm wide GaAs quantum well at 4.2 K, calculated for the same parameters of the excitation. The effective conductivity is expressed in units of σ_0 defined in Sec. III. The

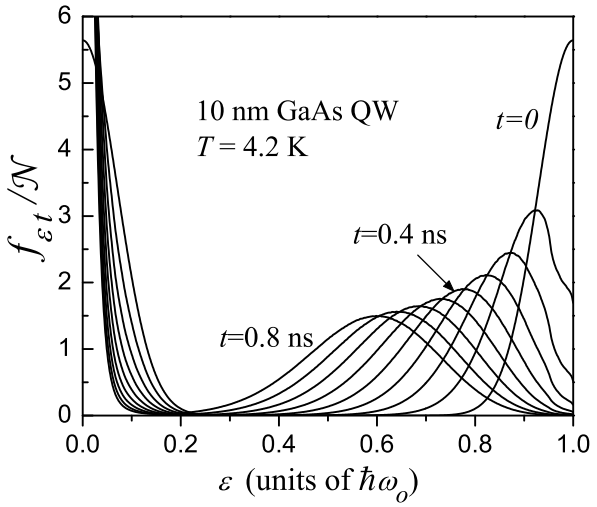

FIG. 4: Temporal evolution of electron energy distribution for the case of initial distribution (20) with $\Delta = 0.1\ \hbar\omega_o$, calculated for 10 nm wide GaAs quantum well at 4.2 K. The distribution functions are plotted with the time interval of 0.1 ns and normalized by $\mathcal{N} = n_{ex}[\rho_{ß2D}\hbar\omega_o]^{-1}$.

temporal dependence of $\sigma_t^{ßeff}$ at zero magnetic field is shown by a dashed line, and is similar to that calculated for bulk samples in Ref. 9. The evolution of $\sigma_t^{ßeff}$ and $E_t^{ß\perp}$ appears to be very sensitive to the cyclotron frequency and characteristic frequency Ω [see Eq. (14)] because of the initial exponential increase of the current and Hall field. We have chosen these frequencies in such a way that the absolute values of $\sigma_t^{ßeff}$ and $E_t^{ß\perp}$ in Fig. 5 are not too large. By varying the parameters, one can obtain a very strong (several orders of magnitude) enhancement of $\sigma_t^{ßeff}$ and $E_t^{ß\perp}$, but the qualitative picture of the damped oscillations remains the same. The increase of the magnetic field leads to increasing frequency of the oscillations, while the amplitude of the oscillations decreases and the relaxation slows down. The increase of the excitation density, which leads to increasing frequency Ω, exponentially increases the amplitude of the oscillations.[12] This influence of the parameters on the evolution is also described by the simple model investigated in the previous section.

The general features of the evolution are not modified if the electrons are excited by a shorter optical pulse, which results in energy broadening of the initial distribution. Figure 6 shows the temporal dependence of $\sigma_t^{ßeff}$ and $E_t^{ß\perp}$ calculated for the case of initial distribution (20) with $\Delta = 0.2\ \hbar\omega_o$. A comparison of this figure to Fig. 5 also demonstrates the increase of the oscillation frequency and a suppression of the damping as a result of the increased Ω (see the discussion of Eq. (17)).

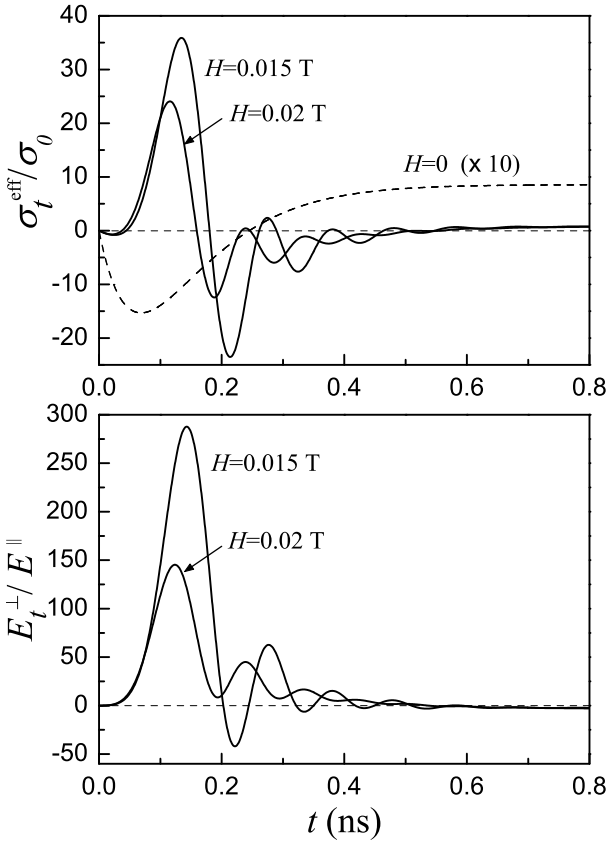

FIG. 5: Evolution of the effective conductivity $\sigma_t^{ßeff}$ and Hall field $E_t^{ß\perp}$ at $\Omega = 50$ ns^{-1} in the magnetic fields $H = 0.015$ T and 0.02 T, for the case of initial distribution (20) with $\Delta = 0.1\ \hbar\omega_o$. The dashed line shows $\sigma_t^{ßeff}$ (multiplied by 10) for zero magnetic field.

V. CONCLUSIONS

We have described the transient classical magnetotransport of electrons in a long Hall bar after ultrafast interband photoexcitation, and calculated the temporal dependence of the current and Hall field. Investigating the modification of the response due to accumulation of the edge charges forming the transverse (Hall) voltage, we have found the oscillations of both the current and the Hall field. The amplitude and duration of the oscillations are dramatically enhanced if the energies of the excited electrons are in the vicinity of the optical phonon energy. This is the case when the oscillations are triggered by the instability associated with the partial inversion of electron distribution (the ANC effect). Although the numerical calculations have been carried out here for non-doped GaAs quantum wells, similar effects should be expected for non-doped bulk samples, because the qualitative features of the energy relaxation and non-local temporal response of electron system do not depend on

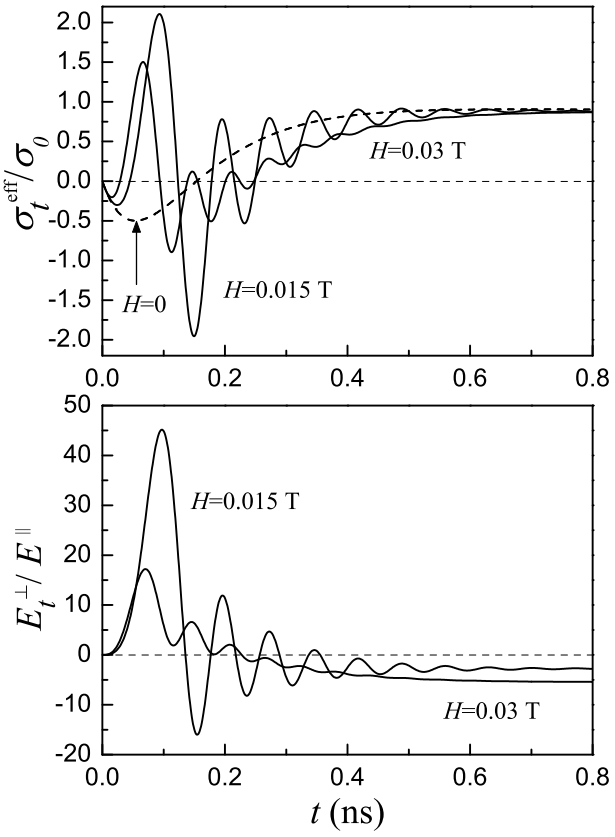

FIG. 6: Evolution of the effective conductivity $\sigma_t^{ßeff}$ and Hall field $E_t^{ß\perp}$ at $\Omega = 80$ ns^{-1} in the magnetic fields $H = 0.015$ T and 0.03 T, for the case of initial distribution (20) with $\Delta = 0.2\ \hbar\omega_o$. The dashed line shows $\sigma_t^{ßeff}$ for zero magnetic field.

dimensionality.

Now we discuss the assumptions used. The main approximation is the consideration of electron scattering by phonon modes only. The elastic scattering by inhomogeneities can be neglected in the case of non-doped quantum wells with high-quality interfaces. In any case, it is not difficult to include this scattering into consideration, because it does not contribute to the energy relaxation (see Eq. (4)), and can lead only to an increase in the momentum relaxation rate standing in Eq. (8). However, the damping of the oscillations in this case becomes stronger, and it is always better to avoid this additional scattering by using clean samples. A more important restriction is the neglect of electron-electron interaction, which should dominate the energy relaxation of photoexcited 2D electrons at the densities $n_{ex} > 10^{10}$ cm^{-2}. Since the electron-electron interaction leads to a faster relaxation, it is expected to shorten the time interval where the exponential increase of the current and Hall

field takes place. However, this interaction cannot cancel the large-amplitude oscillations of the current and Hall field. In this connection, we note that these oscillations have been examined in Sec. III on the basis of a model that is not sensitive to the detailed description of the energy relaxation. The only essential point is the existence of partial inversion of electron distribution during a finite interval of time after the photoexcitation, sufficient for realization of the ANC regime. For this reason, the position and energy broadening of the initial electron distribution, which are determined by the parameters of photoexcitation pulse, appear to be more important than the actual energy relaxation mechanisms.

Let us discuss the other approximations. The general formalism has been based on the classical Boltzmann equation. This is sufficient for the subject of our study, because the intervals of times under consideration considerably exceed the quantum broadening times $\hbar/\varepsilon$, and the magnetic field is weak enough to neglect the Landau quantization. We have ignored the existence of holes created in the valence band by the optical pulse. This is possible because of smallness of the hole mobility, so the contribution of the holes to the transport can be neglected. To describe the momentum relaxation by electron-phonon scattering, we have used the elastic approximation. In quantum wells, this is suitable for description of electrons whose energies ε are much larger than the characteristic energy $\hbar s\pi/a$ associated with phonon momentum normal to the layer (here s is the sound velocity and a is the well width). For typical parameters $s \simeq 5 \times 10^5$ cm/s and $a \simeq 10$ nm, the energy $\hbar s\pi/a$ is around 1 meV. Therefore, the assumed condition is satisfied in our calculations for the photogenerated high-energy electrons which give the main contribution to the conductivity. Next, since we have neglected the transverse inhomogeneity of the currents and fields, the equations (9)-(11) are not applicable for description of electrons in the vicinity of the Hall bar edges. Nevertheless, these equations are valid in the main part of the Hall bar, where the inhomogeneous corrections to the currents and fields are small (see Appendix B).

We also note that in the ANC regime one should consider a possibility for the development of a spatial instability[13] both along and across the Hall bar. Uncovering the conditions for existence and properties of such an instability requires a special investigation based on the formalism of non-homogeneous kinetic equation. The spatially-inhomogeneous electron distribution owing to the ANC effect is essential in the stationary regime, and it is realized for 2D electrons under microwave excitation in the quantizing magnetic field.[7] Nevertheless, since we consider the transient response, one may expect that the results of this paper will

remain valid for the samples of small size, where the spatially-inhomogeneous distribution is not developed during the short interval of time corresponding to the exponential increase of the current and Hall field.

Finally, we would like to point out that the Hall oscillations studied in this paper can be viewed as 2D magnetoplasmons with small wavenumbers determined by the width of the Hall bar. To detect them in experiment, it is necessary to have sub-nanosecond temporal resolution, which is attainable for standard all-electrical measurements. Owing to the strong amplification of the oscillations by the ANC instability, the excitation technique based on the ultrafast optical pump can be applied along with the conventional techniques[14] of magnetoplasmon excitation in 2D layers.

APPENDIX A: RELAXATION RATES

Below we present the expressions for $\nu_\varepsilon^{ß(ac)}$ and $W_{\varepsilon\varepsilon'}$ determining the momentum and energy relaxation of 2D electrons under acoustic-phonon scattering. Both these quantities can be written as the sums of partial contributions caused by the DA and PA mechanisms of interaction. The relaxation rate $\nu_\varepsilon^{ß(ac)}$ is calculated in the elastic approximation:

$$\nu_\varepsilon^{ß(ac)} = \frac{2\pi}{\hbar}\int \frac{d\mathbf{p}'}{(2\pi\hbar)^2}\int_{-\infty}^{\infty}\frac{dq_{ß\perp}}{2\pi}M(q_{ß\perp})(1-\cos\varphi) \times\delta(\varepsilon_p-\varepsilon_{p'})\sum_{i=ßDA,PA}\sum_{\lambda=l,t}\overline{|C_{\lambda\mathbf{Q}}^{ß(i)}|^2}(2N_{\lambda Q}+1), \tag{A1}$$

where $\varepsilon=\varepsilon_p=p^2/2m$, $\mathbf{Q}=(\mathbf{q},q_{ß\perp})$ is the phonon wave vector, $\mathbf{q}=(\mathbf{p}-\mathbf{p}')/\hbar$ is the in-plane component of this vector, φ is the angle between $\mathbf{p}$ and $\mathbf{p}'$, $N_{\lambda Q}$ are the Planck occupation numbers of the longitudinal ($\lambda=l$) and transverse ($\lambda=t$) acoustic phonon modes, and $\overline{|C_{\lambda\mathbf{Q}}^{ß(i)}|^2}$ are the matrix elements of interaction, averaged over the angle of electron momentum $\mathbf{p}$ in the 2D plane. This averaging is essential for the PA interaction, which is sensitive to orientation of the vector $\mathbf{Q}$ with respect to crystallographic axes.[15] In the explicit form,

$$\overline{|C_{\lambda\mathbf{Q}}^{ß(DA)}|^2}=\frac{\hbar\mathcal{D}^2Q}{2\rho s_\lambda}\delta_{\lambda,l} \tag{A2}$$

and

$$\overline{|C_{\lambda\mathbf{Q}}^{ß(PA)}|^2}=\frac{\hbar(eh_{14})^2}{2\rho s_\lambda Q}A_{\lambda\mathbf{Q}}\ , \tag{A3}$$

where s_λ are the sound velocities, ρ is the material density, $\mathcal{D}$ is the deformation-potential constant, and h_{14} is the piezoelectric coefficient. The polarization factors $A_{\lambda\mathbf{Q}}$ for (100)-grown 2D layers are[16]

$$A_{l\mathbf{Q}} = \frac{9}{2}\frac{q_{ß\perp}^2 q^4}{Q^6}\ , \quad A_{t\mathbf{Q}} = 4\frac{q_{ß\perp}^4 q^2}{Q^6} + \frac{1}{2}\frac{q^6}{Q^6}. \tag{A4}$$

Finally, $M(q_{ß\perp}) = |\langle 0|e^{iq_\perp z}|0\rangle|^2$ is the squared matrix element of a plane-wave factor. This matrix element characterizes the interaction of 2D electrons with 3D phonons and depends on the confinement potential determining the ground state of 2D electrons, $|0\rangle$. We apply the model of a deep square well of width a leading to the expression[2] $M(q_{ß\perp}) = [\sin(x)/x]^2/[1-(x/\pi)^2]^2$, where $x = q_{ß\perp}a/2$.

The introduction of the transition probability $W_{\varepsilon\varepsilon'}$ entering Eqs. (2) and (4) implies averaging of the kinetic equation over the angle of momentum $\mathbf{p}$, according to $\partial f_{\varepsilon t}/\partial t = (2\pi)^{-1}\int_0^{2\pi} d\varphi_{\mathbf{p}} \sum_{\mathbf{p}'}(W_{\mathbf{p}'\mathbf{p}} f_{\varepsilon' t} - W_{\mathbf{p}\mathbf{p}'} f_{\varepsilon t})$, where $W_{\mathbf{p}\mathbf{p}'}$ is the probability of electron scattering from the state with momentum $\mathbf{p}$ to the state with momentum $\mathbf{p}'$. As a result,

$$W_{\varepsilon\varepsilon'} = \frac{1}{\hbar^2}\frac{\mathrm{sgn}(\varepsilon-\varepsilon')}{1-\exp[(\varepsilon'-\varepsilon)/T]}$$
$$\times \sum_{i=DA,PA}\sum_{\lambda=l,t}\int_0^{\varphi_\lambda}\frac{d\varphi}{\pi} M(q_{ß\perp})\overline{|C_{\lambda\mathbf{Q}}^{ß(i)}|^2}\frac{Q}{s_\lambda q_{ß\perp}}, \tag{A5}$$

where $\overline{|C_{\lambda\mathbf{Q}}^{ß(i)}|^2}$ and $M(q_{ß\perp})$ are already defined above. However, the wave numbers Q, q, and $q_{ß\perp}$ standing in the corresponding equations should be now considered as functions of energies, phonon polarization, and scattering angle φ, according to $Q = |\varepsilon-\varepsilon'|/\hbar s_\lambda$, $q = \sqrt{2m(\varepsilon+\varepsilon'-2\sqrt{\varepsilon\varepsilon'}\cos\varphi)}/\hbar$, and $q_{ß\perp} = \sqrt{Q^2-q^2}$. The integral over the scattering angle in Eq. (A5) must be calculated numerically. The upper limit of this integration, φ_λ, is determined from the requirement $Q^2 > q^2$, which means $\varphi_\lambda = \pi$ at $(\sqrt{\varepsilon}-\sqrt{\varepsilon'})^2 > 2ms_\lambda^2$ and $\varphi_\lambda = \arccos\left([\varepsilon+\varepsilon'-(\varepsilon-\varepsilon')^2/2ms_\lambda^2]/2\sqrt{\varepsilon\varepsilon'}\right)$ at $(\sqrt{\varepsilon}-\sqrt{\varepsilon'})^2 < 2ms_\lambda^2$. In the case of very small energies, $(\sqrt{\varepsilon}+\sqrt{\varepsilon'})^2 < 2ms_\lambda^2$, the limit φ_λ should be set at zero and the integral gives no contribution.

APPENDIX B: EDGE CHARGE ACCUMULATION

This appendix contains a simple formalism describing inhomogeneous distributions of charges, currents, and fields in a long Hall bar for a time-dependent problem. The homogeneous approximation, which is valid in the central part of the bar and leads to Eq. (11)

for the transverse current describing edge charge accumulation, follows from the general consideration.

Consider a semiconductor structure containing a 2D Hall bar of width d and length L ($-d/2 < y < d/2$ and $-L/2 < x < L/2$) placed at a distance h below the surface of the medium with dielectric permittivity ϵ. If the retardation effects are neglected, the electrostatic potential $\Phi_t(y,z)$ created by the 2D carriers satisfies the Poisson equation

$$\left[\frac{\partial}{\partial z}\epsilon(z)\frac{\partial}{\partial z}+\epsilon(z)\frac{\partial^2}{\partial y^2}\right]\Phi_t(y,z)=-4\pi e\delta n_t(y)\delta(z+h), \tag{B1}$$

where $\epsilon(z)=\epsilon$ at $z<0$, $\epsilon(z)=1$ at $z>0$, $\delta n_t(y)=n_t(y)-p$ is the excess density of free electrons, and p is the density of holes which is assumed to be homogeneous and time-independent (because of low mobility of holes, this is possible in the short time interval under consideration). The Poisson equation is two-dimensional because the bar is long, $d \ll L$, and the electron density depends only on the transverse coordinate y. If $\epsilon \gg 1$, one can use the Newmann's boundary condition $\partial\Phi_t(y,z)/\partial z|_{z=-0}=0$ at the surface and rewrite Eq. (1) in the integral form

$$\Phi_t(y,z)=-\frac{e}{\epsilon}\int_{-d/2}^{d/2}dy'\left[\ln[(y-y')^2+(z+h)^2]+\ln[(y-y')^2+(z-h)^2\right]\delta n_t(y'). \tag{B2}$$

The other necessary equations are the continuity equation

$$e\frac{\partial\delta n_t(y)}{\partial t}+\frac{\partial j_t^{ß\perp}(y)}{\partial y}=0, \tag{B3}$$

which relates the density to the transverse current, and the equation

$$\delta n_t(y)=e\rho_{ß2D}[v_t(y)-\varphi_t(y)], \tag{B4}$$

where $\varphi_t(y)=\Phi_t(y,-h)$ is the electrostatic potential in the 2D plane and $v_t(y)$ is the electrochemical potential. Finally, there is a relation between the transverse current and electrochemical potential,

$$j_t^{ß\perp}(y)=\int_0^t dt'\left(-\sigma_{tt'}^{ß\|}\frac{\partial}{\partial y}v_{t'}(y)+\sigma_{tt'}^{ß\perp}E^{ß\|}\right), \tag{B5}$$

which is a generalization of Eq. (9): $E_{t'}^{ß\perp}$ replaced by $-\partial v_{t'}(y)/\partial y$ in order to take into account the spatial inhomogeneity.

Using Eqs. (B2), (B3), and (B4), one can exclude the electrostatic potential and electron density, and write

$$-\frac{\partial j_t^{ß\perp}(y)}{\partial y}+\frac{2e^2\rho_{ß2D}}{\epsilon}\int_{-d/2}^{d/2}dy'K(y,y')\frac{\partial j_t^{ß\perp}(y')}{\partial y'}=e^2\rho_{ß2D}\frac{\partial v_t(y)}{\partial t}, \tag{B6}$$

where $K(y,y') = \ln|y-y'| + \ln\sqrt{(y-y')^2+(2h)^2}$. Equations (B5) and (B6), with the boundary condition $j_t^{ß\perp}(\pm d/2) = 0$, give a complete description of the spatial distribution of transverse current and electrochemical potential in the long Hall bar. The spatial inhomogeneity is essential near the edges $\pm d/2$, this follows from the fact that the transverse current goes to zero at $y = \pm d/2$. On the other hand, in the main part of the bar one should expect nearly homogeneous currents and fields. If the bar width d is large in comparison to the Bohr radius $\hbar^2\epsilon/e^2m$, the main contribution to the right-hand side of Eq. (B6) comes from the integral term, which is written after integration by parts as $(2e^2\rho_{ß2D}/\epsilon)\int_{-d/2}^{d/2} dy'[\partial K(y,y')/\partial y] j_t^{ß\perp}(y')$. Let us search for the solution of Eq. (B6) in the form $j_t^{ß\perp}(y) = j_t^{ß\perp} + \delta j_t(y)$, where $j_t^{ß\perp}$ is the homogeneous part of the current and $\delta j_t(y)$ is the inhomogeneous correction. Neglecting first $\delta j_t(y)$ (zero-order iteration), we obtain $j_t^{ß\perp} = \epsilon\{2[K(y,-d/2) - K(y,d/2)]\}^{-1}[\partial v_t(y)/\partial t]$, which is rewritten, under the reasonable assumption $d \gg 4h$, as

$$j_t^{ß\perp} = \frac{\epsilon}{4\ln|(d/2+y)/(d/2-y)|}\frac{\partial v_t(y)}{\partial t}. \tag{B7}$$

Generally speaking, this equation can be satisfied for all y if the transverse field is inhomogeneous. In other words, $v_t(y) = -E_t^{ß\perp} y + \delta v_t(y)$, where $\delta v_t(y)$ is the inhomogeneous correction to the electrochemical potential. However, in the central part of the sample, where $\ln|(d/2+y)/(d/2-y)| \simeq 4y/d + O[(y/d)^3]$, the inhomogeneous correction $\delta v_t(y)$ can be neglected and the electrochemical potential is expressed through the homogeneous transverse field, $v_t(y) \simeq -E_t^{ß\perp} y$. Equation (B7) in these conditions is reduced to Eq. (11) with the effective capacitance $C_{ß\perp} = \epsilon d/16$ (so the coefficient α introduced after Eq. (11) is equal to 1/16), while Eq. (B5) is reduced to Eq. (9). Using these solutions, one can write an equation for the inhomogeneous correction to the current (first-order iteration), which shows that the relative contribution of $\delta j_t(y)$ is small, $d^{-1}\int_{-d/2}^{d/2} dy\,\delta j_t(y) \ll j_t^{ß\perp}$, this smallness is of numerical origin. Therefore, the homogeneous approximation described by Eqs. (9) and (11) is justified.

---

[1] V. F. Gantmakher and I. B. Levinson, *Carrier Scattering in Metals and Semiconductors* (Elsevier Sci. Ltd., New York, 1987).

[2] P. J. Price, Ann. Phys. **133**, 217 (1981).

[3] T. Yao, K. Inagaki, and S. Maekawa, in *Proceedings of the 11th International Conference on the Physics of Semiconductors* (Polish Scientific Publishers, Warszawa, 1972), Vol. 1, p. 417.

[4] P. G. Harper, J. W. Hodby, and R. A. Stradling, Rep. Prog. Phys. 36, 1 (1973).

[5] H. J. Stocker, Phys. Rev. Lett. **18**, 1197 (1967); V. F. Elesin and V. A. Manykin, Pis'ma Zh. Eksp. Teor. Fiz. 3, 26 (1966) [JETP Lett. **3**, 15 (1966)]; Zh. Eksp. Teor. Fiz. 50, 1381 (1966) [Sov. Phys. JETP **23**, 917 (1966)].

[6] E. Erlbach, Phys. Rev. **132**, 1976 (1963).

[7] R. Fitzgerald, Phys. Today **56**, 24 (2003); A. C. Durst and S. H. Girvin, Science **304**, 1762 (2004); V. I. Ryzhii, Physics - Uspekhi **48**, 205 (2005); S. I. Dorozhkin, Physics - Uspekhi **48**, 213 (2005).

[8] F. T. Vasko, Pis'ma Zh. Eksp. Teor. Fiz. 79, 539 (2004) [JETP Lett., **79**, 431 (2004)].

[9] O. E. Raichev and F. T. Vasko, Phys. Rev. B **73**, 075204 (2006).

[10] F. T. Vasko and O. E. Raichev, *Quantum Kinetic Theory and Applications* (Springer, New York, 2005).

[11] I. Vurgaftman, J.R. Meyer, and L.R. Ram-Mohan, J. Appl. Phys. **89**, 5815 (2001).

[12] It is interesting to note that a complete neglect of the retardation of edge charging, formally corresponding to $\Omega \to \infty$, would lead to a hyperbolic singularity in the temporal dependence of the Hall field. The analytical solution of Eq. (14) in this case is $E_t^{ß\perp}/E^{ß\|} = -(\omega_c/g_t)\int_0^t dt' e^{-\nu(t-t')} g_{t'}$, and the Hall field diverges when the factor g_t changes its sign from negative to positive.

[13] E. Scholl, *Nonequilibrium Phase Transitions in Semiconductors* (Springer, Berlin, 1987).

[14] E. Batke, D. Heitmann, and C. W. Tu, Phys. Rev. B **34**, 6951 (1986).

[15] J. D. Zook, Phys. Rev. **136**, A869 (1964).

[16] V. Karpus, Semicond. Sci. Technol. **5**, 691 (1990).